Silicon-based nanoelectronic field-effect *p*H sensor with local gate control

Yu Chen, Xihua Wang, Shyamsunder Erramilli, and Pritiraj Mohanty[a)]
Department of Physics, Boston University, 590 Commonwealth Avenue, Boston, Massachusetts 02215

Agnieszka Kalinowski
School of Medicine, Carnegie Mellon University and University of Pittsburgh, Pittsburgh, Pennsylvania 15261

(Received 24 August 2006; accepted 6 October 2006; published online 29 November 2006)

The authors demonstrate the operation of a nanoscale field-effect *p*H sensor engineered from a functionalized silicon nanowire. With this nanofabricated *p*H sensor, the change in the hydrogen ion concentration or the *p*H value of a solution can be detected by the corresponding change in the nanowire differential conductance with a resolution of ±5nS/*p*H. Fabrication of selective side gates on the nanowire sensor allows field-effect control of the surface charge on the nanowire by controlling the accumulation of charge carriers with the side-gate voltage. A simple physical model is used to analyze the observed data and to quantify the dependence of the conductance on *p*H. The development of a nanoscale sensor with physically engineered gates offers the possibility of highly parallel labeling and detection of chemical and biological molecules with selective control of individual array elements. © *2006 American Institute of Physics*. [DOI: 10.1063/1.2392828]

Ultrasensitive detection of biological and chemical species is fundamental to the screening and detection of disease, discovery and screening of drugs, as well as gas detection and biomolecular analysis.[1,2] In particular, the ability to detect ions in liquid solutions with ion-selective nanoscale electronic sensors is attractive to a number of fields. For instance, in addition to the detection of proteins, virus, and DNA,[3–6] biocompatible silicon-based sensors have been used for *in vivo* neurological studies such as the detection of calcium and potassium ion concentrations. Furthermore, highly parallel detection by an array of such sensors with control over individual elements offers the possibility of advanced engineering for enhancement in detection sensitivity as well as simultaneous analysis of multiple species.

Nanostructures such as nanowires,[7] nanotubes,[8] nanocrystals,[9] nanocantilevers,[10] and quantum dots[11] are particularly attractive as biosensors, since the critical dimensions of the nanostructures, such as the diameter of the nanowire, are comparable to the sizes of biological and chemical species. The detection sensitivity is therefore greatly enhanced as the signal can be effectively transduced because of large surface-to-volume ratio. In a nanoscale conductor, the surface-to-volume ratio is large because of size, so its electrical property such as conductance is dominated by surface contributions. Therefore, the presence of charged proteins on the surface of an active nanowire induces a large fractional change in the nanowire conductance and enables relatively easy detection.

A silicon nanowire can be used as an ultrasensitive detector by taking advantage of the field effect. A conventional silicon nanowire can be used as a sensor of hydrogen ion concentration or a *p*H sensor by modifying its surface with 3-aminopropyltriethoxysilane (APTES), which produces amino groups as well as silanol (Si–OH) groups on the nanowire surface. These groups operate as receptors of hydrogen ions, which undergo protonation/deprotonation reactions. In the process, the surface charge on the silicon nanowire changes, which, in turn, changes the nanowire conductance. In an *n*-type silicon nanowire, with increasing *p*H, there is an increase in the negative charge on the surface, which acts like a negatively charged gate. This causes the channel of the charge carrier to deplete, therefore the net conductance decreases. The accumulation of carriers by the reception of hydrogen ions can be viewed as a field effect as it modulates the *n*-type field-effect transistor (FET) device.

In a pioneering experiment, Cui *et al.*[7] have demonstrated the operation of a nanoelectronic *p*H sensor fabricated with a "bottom-up" method. The change in the nanowire conductance as a function of *p*H was found to be consistent with the previous measurements of *p*H-dependent surface charge density on silica.[12] The silicon nanowires could be further aligned by a vapor-liquid-solid growth flow technique[13] along the electrodes. Further experiments demonstrated the ability of such sensors to detect biological species such as proteins[3] and virus molecules.[5] Additional control on the conductance of the functionalized FET devices was obtained with the application of a gate voltage to the substrate.

In a fundamentally different approach to device architecture, here we demonstrate the operation of a nanoelectronic *p*H sensor fabricated with a "top-down" method. The essential advantage of this approach is the complete control over physical and electronic degrees of freedom. The geometry and alignment of the nanowire can be fully controlled by e-beam lithography and standard semiconductor processing techniques. Furthermore, physical gate electrodes next to the nanowire can be fabricated with complete control over their location and size. These local gate electrodes enable controlled accumulation or depletion of surface charge carriers on the nanowire and provide the ability to tune the nanowire conductance necessary for the optimization of the detection sensitivity. In this configuration, the nanowire *p*H sensor regains the control and the benefits, usual in standard electronic FET devices.

The engineering of our device consists of two fundamental steps: fabrication and functionalization. The silicon nano-

[a)]Electronic mail: mohanty@buphy.bu.edu

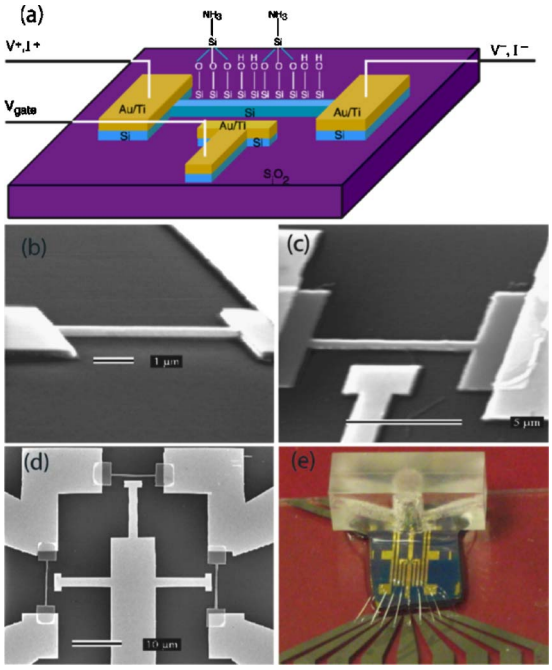

FIG. 1. (Color online) Device schematic diagram, scanning electron micrographs. (a) The schematic diagram of the silicon nanowire with side gates and electrodes. The nanowire is exposed on three sides along the longitudinal direction. (b) The nanowire shown here is 300 nm wide, 230 nm thick, and 8 μm long. (c) A silicon nanowire with a Au/Ti side gate. (d) The scanning electron micrograph displays three silicon nanowire devices on the same chip. (e) An optical micrograph shows the flow chamber sealed on top of the devices on the interface board.

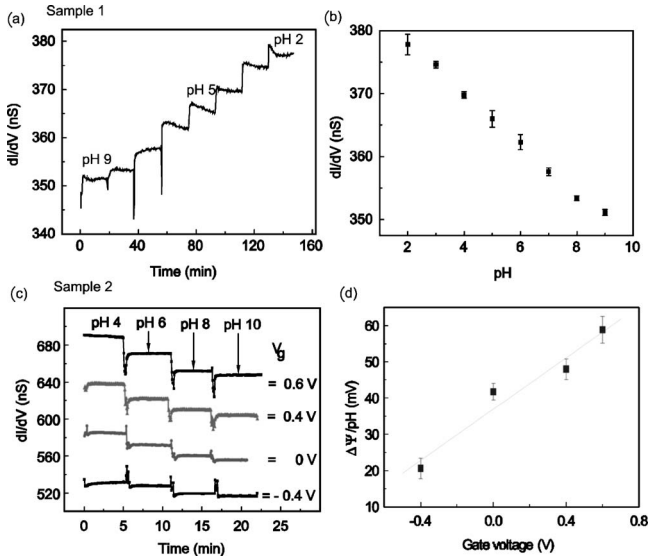

FIG. 2. Zero-bias differential conductance (dI/dV) measurements in solution with different pH values. (a) dI/dV versus time for sample 1, (b) dI/dV versus pH. (c) Zero-bias differential conductance (dI/dV) with increasing pH values of the solution at different gate voltages for sample 2. (d) Effective surface potential change at different gate voltages. The data points for V_g=0.6 V are shifted by 40 nS for clarity in Figs. 2(c). The measurements are done with an ac drive at 37 Hz with an amplitude of 50 mV.

wires along with the side gates and the electrodes are fabricated by standard electron-beam lithography and surface nanomachining. The starting silicon-on-insulator (SOI) wafer has a device-layer thickness of 230 nm and oxide layer thickness of 370 nm with a starting device-layer volume resistivity of 10–20 Ω cm. The device-layer resistivity can be further controlled by doping the wafer by ion implantation of boron with a concentration of $1\times10^{18}/\mathrm{cm}^3$. After patterning the nanowires and the electrodes in separate steps with separate masks, the structure is etched out with an anisotropic reactive-ion etch. This process exposes the three surfaces of the silicon nanowire along the longitudinal direction as shown in the schematic diagram in Fig. 1(a). After the fabrication of the silicon nanowire and the gold electrodes and gates, a protective layer of polymethylmethacrylate (PMMA) is spun on the surface and only the silicon nanowire is exposed by a secondary e-beam exposure, while the device floor of oxide remains covered. This process allows exposure of only the silicon nanowire to air/solution. The functionalization of the nanowire surface is done by the application of a 2% APTES solution of methanol for 3 h. After multiple rinsing of the device by methanol, the device is dried by nitrogen gas and baked at 80 °C in an oven for 10 min. Following this APTES functionalization technique, the plastic flow chamber is attached to the device with the application of PMMA and silicone gel [Fig. 1(e)]. The flow chamber is designed to include inlet and outlet tubes, connected to a syringe pump, to allow solution flow over the functionalized nanowire inside the chamber. The volume of the flow chamber is estimated to be ~35 μl.

Measurement of pH-dependent conductance in presence of solution is carried out in two separate methods. One method is the standard two-probe I-V measurement of the nanowire along with a gate voltage applied to one of the side gates shown in Fig. 1(c). Because of the high resistance of the nanowire, the I-V characteristic is measured with a Keithley 2400 source meter with a current resolution of 10 pA. Additionally, an Agilent 4339B high-impedance bridge is used for calibration and comparison. In order to discern small changes in the pH-dependent conductance, we have used another more elaborate technique of differential conductance (dI/dV) measurement. The measurement circuit includes a small ac modulation (provided by an EG&G 5210 lock-in amplifier), superimposed on the dc bias across the nanowire (provided by the Keithley 2400 source meter). The ac modulation and the dc bias are added by a noninverting summing circuit, which is integrated with the preamplifier circuit. The circuit is then put in a rf-shielded aluminum box to prevent noise pickup. Differential conductance measurements are done by sweeping the dc bias at a constant ac modulation amplitude and measuring the response with the lock-in amplifier, referenced to the ac signal frequency. This approach allows the measurement of zero-bias conductance $dI/dV|_{V=0}$, avoiding bias-dependent effects in the solution such as electrolysis.

Figure 2 displays zero-bias differential conductance of the functionalized nanowire in pH solution. The wire is 300 nm wide, 230 nm thick, and 8 μm. Solutions with varying hydrogen ion concentration or pH are made from phosphate buffered saline, containing 10 mM of phosphate and 130 mM of NaCl. The zero-bias conductance of the nanowire increases with increasing pH. Figures 2(a) and 2(b) show an almost linear relation between dI/dV and pH value of the solution. Further evidence of field effect is demonstrated by zero-bias conductance measurement at different gate voltages, shown in Fig. 2(c). All the measurements are done at room temperature. The zero-bias conductance is tuned by the application of the side-gate voltage. A positive gate bias implies opening of the charge carrier channel, simi-

lar to the inversion layer in silicon devices. A negative gate bias implies depletion or squeezing of the charge carrier channel, similar to depletion layer. The zero-bias conductance increases or decreases depending on positive or negative gate bias, respectively.

Field-effect transistors constitute a rich area of semiconductor physics. The term "FET" covers a large family of devices, which include metal-oxide FET (also called insulated gate field-effect transistor), junction field-effect transistors (JFETs), and so on. It is not clear which model best describes the operation of gated silicon nanowires in solution. The detailed description, as well as the functional dependence of device characteristics on external controls, is different. It is advantageous to describe the operation of the nanowire device in terms of directly measurable experimental quantities of interest.

Our model for interpreting the nanoscale devices in this study is based on a JFET, but with the device characteristics that depend on solution *p*H and ionic strength. Larger scale devices used for ion sensitive measurements are called "ion-selective field-effect transistors" (ISFETs).[14] An explicit comparison with ISFETs may be made by considering the threshold voltage, which determines the current flow in the silicon wire as[14]

$$V_t = V_0 - \Psi, \tag{1}$$

where Ψ is the effective surface potential which is a function of *p*H, the constant V_0, and the ionic charge q

$$\Delta\Psi = -2.3\alpha\frac{kT}{q}\Delta p\mathrm{H}_{\mathrm{bulk}}. \tag{2}$$

The sensitivity factor α depends on the geometry and nature of the device and environmental factors such as temperature. It ranges between 0 and 1. Equation (2) suggests that the temperature dependence of the surface potential is complicated. Furthermore, large changes in temperature also strongly influence transport properties of the semiconductor. A detailed study of temperature effects needs to take into account the effect on the concentration and mobility of charge carriers in the semiconductor, the effect of phonons. For ion sensing in aqueous solvents, we restrict our study here to room temperature (T=298 K). Under these conditions, when α=1,

$$\frac{\Delta\Psi}{\Delta p\mathrm{H}_{\mathrm{bulk}}} = -2.3\alpha\frac{kT}{q} = \sim -60\ \mathrm{mV}. \tag{3}$$

For our device, we consider the conduction channel to be the central region of the nanowire with a depletion region between the channel and the naturally formed SiO_2 surface. When *p*H of the solution is changed, protonation or deprotonation of the APTES modified surface can change the thickness of the depletion region. So the conductance of the wire changes. This is similar to the operation principle of JFET. However, the wire is in nanoscale. Higher surface-to-volume ratio of the smaller wire can give better sensitivity. Adding different gate voltages shares the same principle of extending or squeezing the conduction channel. So the sensitivity can be improved by adding suitable gate voltage.

In the differential conductance measurement at zero bias, the conductance change due to *p*H is 5 nS/*p*H at V_g=0 V, and the conductance change due to gate voltage is 130 nS/V at *p*H=8. After calibration from these quantities, effective surface potential change $\Delta\Psi$ is 20 mV/*p*H at V_g=−0.4 V and 60 mV/*p*H at V_g=0.6 V as shown in Fig. 2(d).

Further enhancement of sensitivity of our sensors can be done by reducing the dimensions of the silicon nanowire to increase the effective surface-to-volume ratio, reducing the doping concentration of the starting SOI wafer for optimized conductance, creating a better Ohmic contact between the electrodes and the underlying silicon surface by local doping, and optimizing the flow-chamber design for faster throughput.

In conclusion, we demonstrate fabrication, functionalization, and operation of a nanoelectronic field-effect *p*H sensor. The physically engineered silicon nanowire with side gates is fabricated with standard semiconductor processing techniques. The functionalized silicon nanowire can be controlled with local nanoscale side gates to induce inversion or depletion layers. Our approach offers the possibility of highly parallel detection of ion or charged protein and DNA with local control of individual elements. By selective gating, individual nanowires in an array can be turned on or off during functionalization. Therefore the array can contain multiple receptors for the simultaneous detection of multiple chemical and biological species in a single integrated chip.

The authors acknowledge support by the Department of Defense MSRP program (W81XWH-04-1-0578) and the National Science Foundation (DBI-0242697). One of the authors (X.W.) acknowledges support from a Fellowship at the Center for Photonics, Boston University. The authors thank Rostem Irani, Jiandi Wan, Eric Pennick, and David Osborne for invaluable help and discussion.

[1] M. Ferrari, Nature (London) **5**, 161 (2005).
[2] P. Bergveld, IEEE Trans. Biomed. Eng. **19**, 342 (1972).
[3] F. Patolsky, G. Zheng, and C. M. Lieber, Anal. Chem. **78**, 4260 (2006).
[4] W. U. Wang, C. Chen, K. Lin, Y. Fang, and C. M. Lieber, Proc. Natl. Acad. Sci. U.S.A. **102**, 3208 (2005).
[5] Z. Li, B. Rajendran, T. I. Kamins, X. Li, Y. Chen, and R. S. Williams, Appl. Phys. A: Mater. Sci. Process. **80**, 1257 (2005).
[6] F. Patolsky, G. Zheng, O. Hayden, M. Lakadamyali, X. Zhuang, and C. M. Lieber, Proc. Natl. Acad. Sci. U.S.A. **101**, 14017 (2004).
[7] Y. Cui, Q. Wei, H. Park, and C. M. Lieber, Science **293**, 17 (2001).
[8] P. G. Collins, K. Bradley, M. Ishigami, and A. Zettl, Science **287**, 1801 (2000); R. J. Chen, S. Bangsaruntip, K. A. Drouvalakis, N. W. S. Kam, M. Shim, Y. Li, W. Kim, P. J. Utz, and H. Dai, Proc. Natl. Acad. Sci. U.S.A. **100**, 4984 (2003).
[9] Y. X. Liang, Y. J. Chen, and T. H. Wang, Appl. Phys. Lett. **85**, 666 (2004); V. C. Sanz, M. L. Mena, A. Gonzalez-Cortes, P. Yanez-Sedeno, and J. M. Pingarron, Anal. Chim. Acta **528**, 1 (2005).
[10] S. R. Manalis, E. B. Cooper, P. F. Indermuhle, P. Keernen, P. Wagner, D. G. Hafeman, S. C. Minne, and C. F. Quate, Appl. Phys. Lett. **76**, 1072 (2000); L. Johnson, A. K. Gupta, A. Ghafoor, D. Akin, and R. Bashir, Sens. Actuators B **115**, 189 (2006); G. Wu, R. H. Datar, K. M. Hansen, T. Thundat, R. J. Cote, and A. Majumdar, Nat. Biotechnol. **19**, 856 (2001).
[11] W. C. W. Chan, and S. Nie, Science **281**, 2016 (1998); D. R. Larson, W. R. Zipfel, R. M. Williams, S. W. Clark, M. P. Bruchez, F. W. Wise, and W. W. Webb, *ibid.* **300**, 1434 (2003).
[12] G. H. Bolt, J. Phys. Chem. **61**, 1166 (1957).
[13] Y. Huang, X. Duan, Q. Wei, and C. M. Lieber, Science **291**, 630 (2001).
[14] P. Bergveld, Sens. Actuators B **88**, 1 (2003).